

## Supporting Information

### **An Efficient Non-Reaction Based Colorimetric and Fluorescent Probe for Highly Selective Discrimination of Pd<sup>0</sup> and Pd<sup>2+</sup> in Aqueous Media**

Lubna Rasheed,<sup>a</sup> Muhammad Yousuf,<sup>a</sup> Il-Seung Youn,<sup>a</sup> Genggengwo Shi,<sup>a,b</sup> and Kwang S. Kim<sup>\*,a</sup>

<sup>a</sup>Center for Superfunctional Materials, Department of Chemistry, Ulsan National Institute of Science and Technology (UNIST), Ulsan 44919, Korea

\*Ulsan National Institute of Science and Technology (UNIST)

Ulsan 44919, Korea

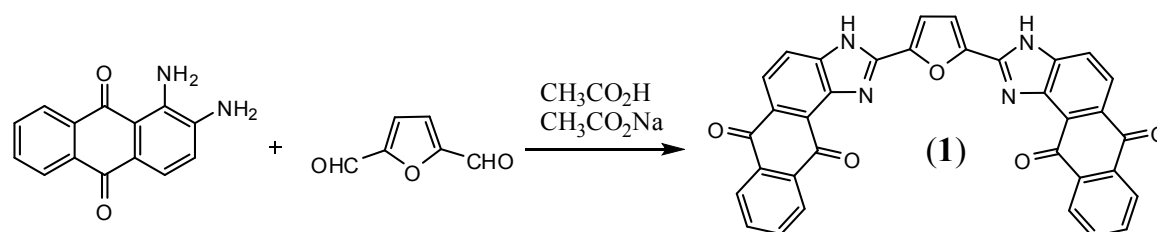
Phone : + 82-52-217-5410, Fax: +82-52-217-5419

Email : [kimks@unist.ac.kr](mailto:kimks@unist.ac.kr) (ksk)

## 1. Experimental techniques:

### General consideration:

The synthesized compounds were fully characterized with standard spectroscopic techniques. Microanalyses were performed on a Carlo 1102 elemental analysis instrument. Electronic absorption (UV-Vis) spectra were recorded using a Shanghai 756 MC UV-Vis spectrometer.  $^1\text{H}$  NMR and  $^{13}\text{C}$  NMR spectra were performed on an Agilent (400 MHz) spectrometer at 298 K. High resolution mass spectra were obtained on a Micromass Platform II mass spectrometer. Fluorescence studies were carried out on Shimadzu RF-5301 PC spectrofluorophotometer at 298 K. 1,2-diamino-anthraquinone, furan-2,5-dicarbaldehyde, sodium acetate and acetic acid were purchased from Aldrich and were used without further purification. Nitrate salts of  $\text{Ca}^{2+}$ ,  $\text{Cd}^{2+}$ ,  $\text{Co}^{2+}$ ,  $\text{Cr}^{3+}$ ,  $\text{Cu}^{2+}$ ,  $\text{Fe}^{2+}$ ,  $\text{Fe}^{3+}$ ,  $\text{Hg}^{1+}$ ,  $\text{Hg}^{2+}$ ,  $\text{K}^{1+}$ ,  $\text{Li}^{1+}$ ,  $\text{Mg}^{2+}$ ,  $\text{Mn}^{2+}$ ,  $\text{Na}^{1+}$ ,  $\text{Ni}^{2+}$ ,  $\text{Pb}^{2+}$ ,  $\text{Pt}^{2+}$ ,  $\text{Zn}^{2+}$ ,  $\text{Zr}^{2+}$ ,  $\text{Ba}^{2+}$ ,  $\text{Ag}^{1+}$ ,  $\text{PdCl}_2$ ,  $\text{AuCl}_3$  and  $\text{Pd}(\text{PPh}_3)_4$  were also purchased from Aldrich and used without further purification.



### Scheme S1. Synthesis of **1**

#### Synthesis of Probe (**1**)

A solution of 1,2-diamino-anthraquinone (238 mg, 1 mmol) in 10 mL acetic acid, sodium acetate (106 mg, 1.3 mmol) and the furan-2,5-dicarbaldehyde were stirred in reflux. TLC was used to monitor the end of the reaction. After the addition of water, the formed precipitate was filtered, and the product was purified by column chromatography using an eluent as a mixture of dichloromethane/ethyl acetate with the ratio 5:1.  $^1\text{H}$  NMR (400 MHz,  $(\text{CD}_3)_2\text{SO}$ , 25°C)  $\delta$  7.77 (d, 2H, furan ring), 7.96 (m, 4H), 8.12 (m, 2H), 8.14 (m, 2H), 8.23 (m, 4H), 9.80 (s, 2H, imidazole);  $^{13}\text{C}$  NMR (100 MHz,  $(\text{CD}_3)_2\text{SO}$ , 25°C)  $\delta$  120.7, 121.5, 126.6, 126.7, 127.2, 127.2, 133.5, 133.5, 134.7, 134.8, 134.9, 153.3, 179.3; Anal. Calcd for  $\text{C}_{34}\text{H}_{16}\text{N}_4\text{O}_5$ : C, 72.86; H, 2.88; N, 10.00, Found: C, 71.96; H, 2.93; N, 10.12. MS(FAB, m/z):  $[\text{M}]^+$  calc.: 560.11; found: 560.10.

## 2. NMR spectral analysis:

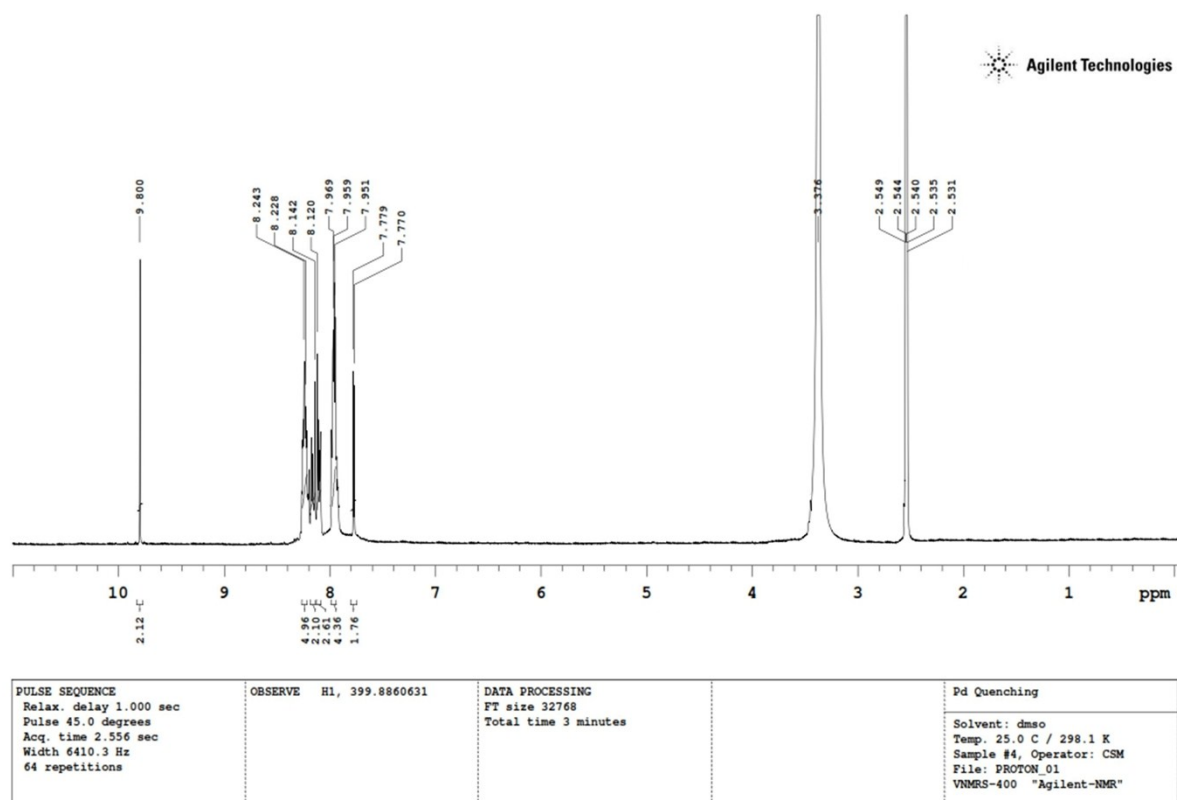


**Figure S1.**  $^1\text{H}$  NMR spectrum of Probe (1) in  $\text{DMSO}-d_6$ .

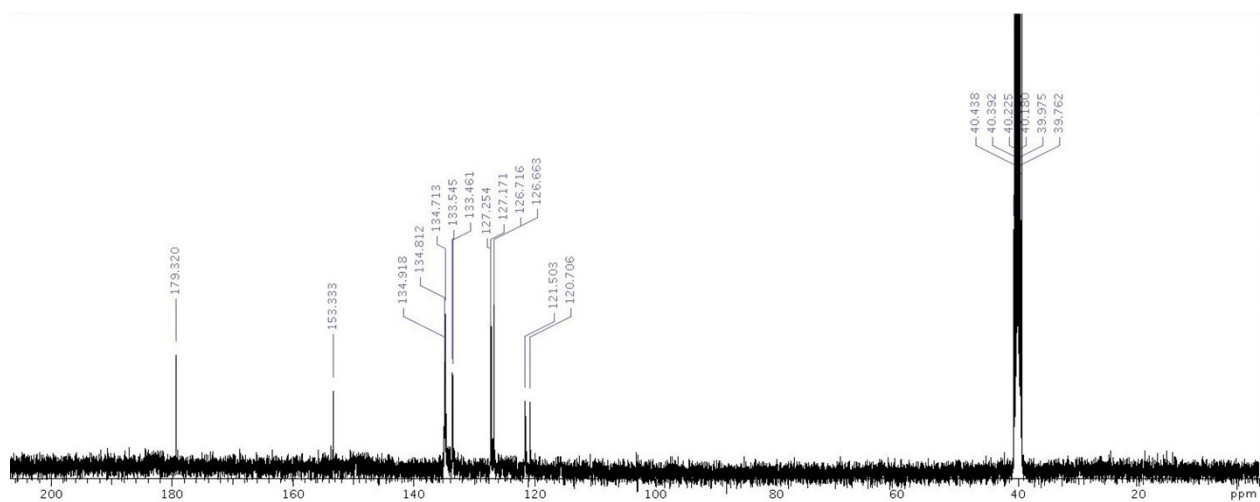


**Figure S2.**  $^{13}\text{C}$  NMR spectrum of Probe (1) in  $\text{DMSO}-d_6$ .

## $^1\text{H}$ NMR titration experiment of probe 1

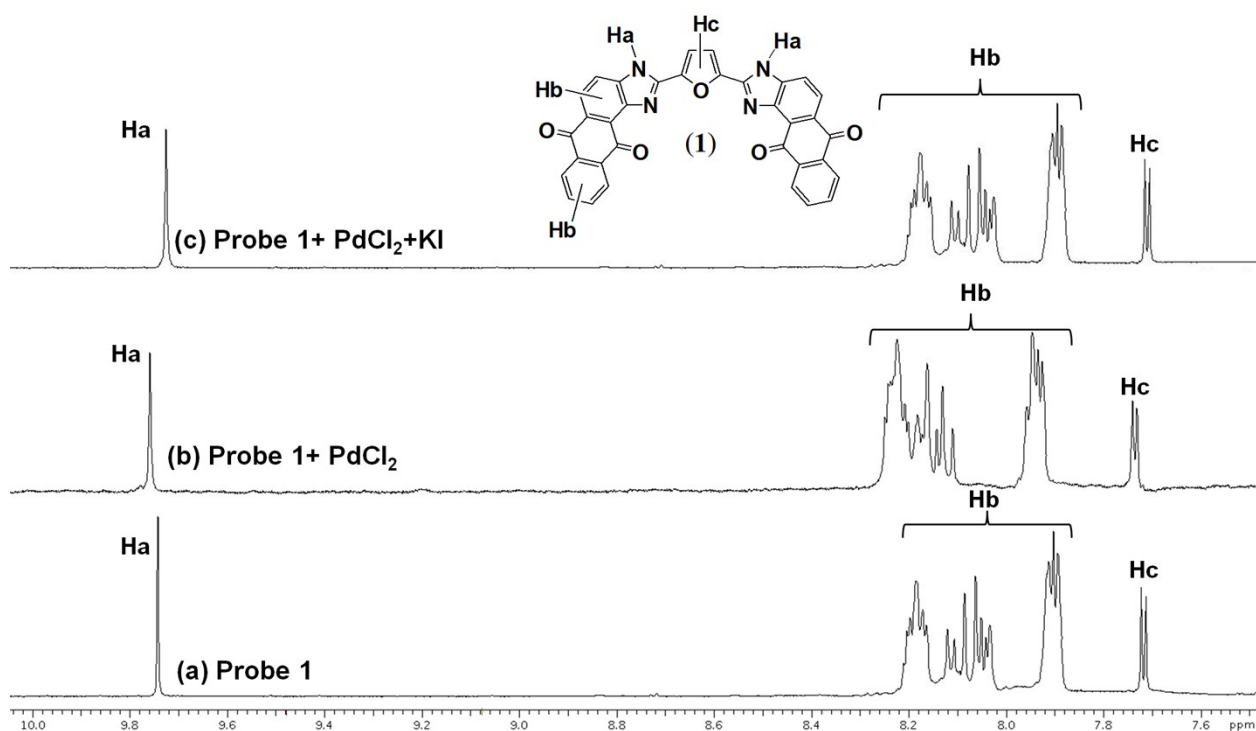


**Figure S3.**  $^1\text{H}$  NMR Probe 1 with and without  $\text{Pd}^{2+}$  ( $\text{DMSO}-d_6$ ) and addition of KI.

### 3. Fluorometric Analysis:

All spectrofluorimetric titrations were performed as follows. Stock solution of compound (1) (1mM) was prepared in ethanol and then diluted to  $10\mu\text{M}$  in 0.01 M HEPES buffer water mixture at pH 7.4 (1:1  $\text{H}_2\text{O}$  and Ethanol). Aliquots of nitrate salts of  $\text{Ca}^{2+}$ ,  $\text{Cd}^{2+}$ ,  $\text{Co}^{2+}$ ,  $\text{Cr}^{3+}$ ,  $\text{Cu}^{2+}$ ,  $\text{Fe}^{2+}$ ,  $\text{Fe}^{3+}$ ,  $\text{Hg}^{1+}$ ,  $\text{Hg}^{2+}$ ,  $\text{K}^{1+}$ ,  $\text{Li}^{1+}$ ,  $\text{Mg}^{2+}$ ,  $\text{Mn}^{2+}$ ,  $\text{Na}^{1+}$ ,  $\text{Ni}^{2+}$ ,  $\text{Pb}^{2+}$ ,  $\text{Pt}^{2+}$ ,  $\text{Zn}^{2+}$ ,  $\text{Zr}^{2+}$ ,  $\text{Ba}^{2+}$ ,  $\text{Ag}^{1+}$ ,  $\text{PdCl}_2$ ,  $\text{AuCl}_3$  and  $\text{Pd}(\text{PPh}_3)_4$  in 0.01 M HEPES buffer water mixture (1:1  $\text{H}_2\text{O}$  and Ethanol)<sup>1</sup> was then injected into the sample solution through a rubber septum in the cap. To account for dilution effects, these stock cation solutions also contained the receptors at its initial concentration. The sample solutions were magnetically stirred for 1 minute after each addition before rescanning. This process was repeated until the change in fluorescence intensity became insignificant. Binding constants  $K_a$  for anions were derived from the plots of  $F/F_0$  vs [cation] by assuming one site model using Origin Lab 8.0.<sup>2</sup> Results reported in the main text are the average of at least three independent titrations. Emission spectrum was measured by keeping slit width = 3 nm and  $\lambda_{\text{exc}} = 425$  nm.

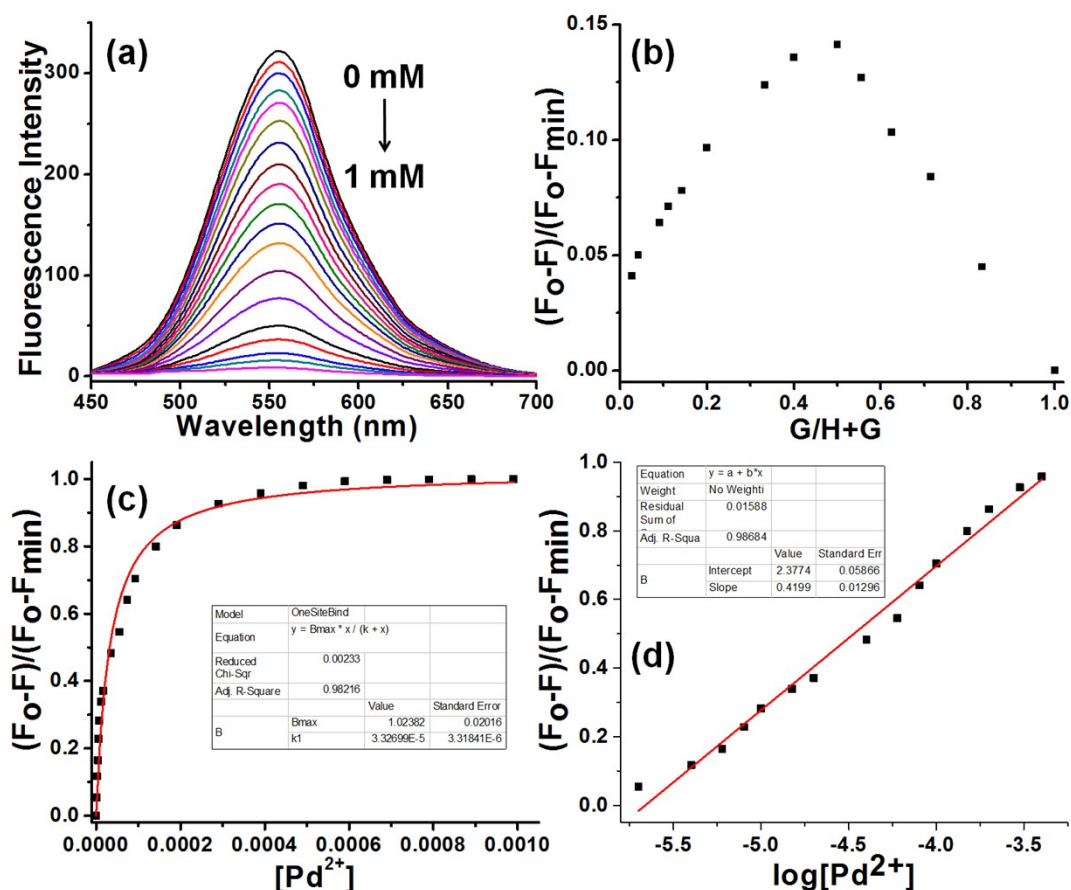


**Figure S4.** (a) Emission spectra (excitation at 425 nm) of receptor **1** (10 μM) upon addition of chloride salt of Pd<sup>2+</sup> at pH 7.4 (0.01 M HEPES buffer, 25°C). (b) Assessment of the stoichiometry of the Pd<sup>2+</sup> complex of **1** via Job plot analysis; [1] + [Pd<sup>2+</sup>] = 10 μM, pH 7.4 (0.01 M HEPES buffer), 25°C. (c) Corresponding binding isotherm. (d) A plot of (F<sub>o</sub>-F)/(F<sub>o</sub>-F<sub>min</sub>) vs log[Pd<sup>2+</sup>].

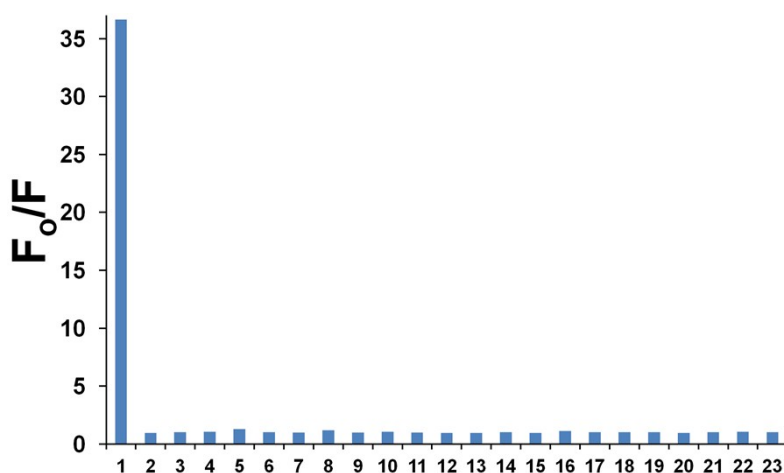


**Figure S5.** Competitive fluorescence response of **1** to various cations at pH 7.4 (0.01M HEPES) (excitation at 425 nm). Bars represent the addition of 10 equivalent of the Pd<sup>2+</sup> and appropriate cation to 10 μM solution of **1** (1:1 H<sub>2</sub>O and Ethanol). (1) No cation, (2) Ca<sup>2+</sup>, (3) Cd<sup>2+</sup>, (4) Co<sup>2+</sup>, (5) Cr<sup>3+</sup>, (6) Cu<sup>2+</sup>, (7) Fe<sup>2+</sup>, (8) Fe<sup>3+</sup>, (9) Hg<sup>1+</sup>, (10) Hg<sup>2+</sup>, (11) K<sup>+</sup>, (12) Li<sup>+</sup>, (13) Mg<sup>2+</sup>, (14) Mn<sup>2+</sup>, (15) Na<sup>+</sup>, (16) Ni<sup>2+</sup>, (17) Pb<sup>2+</sup>, (18) Pt<sup>2+</sup>, (19) Zn<sup>2+</sup>, (20) Zr<sup>2+</sup>, (21) Ba<sup>2+</sup>, (22) Au<sup>1+</sup> and (23) Ag<sup>1+</sup>.

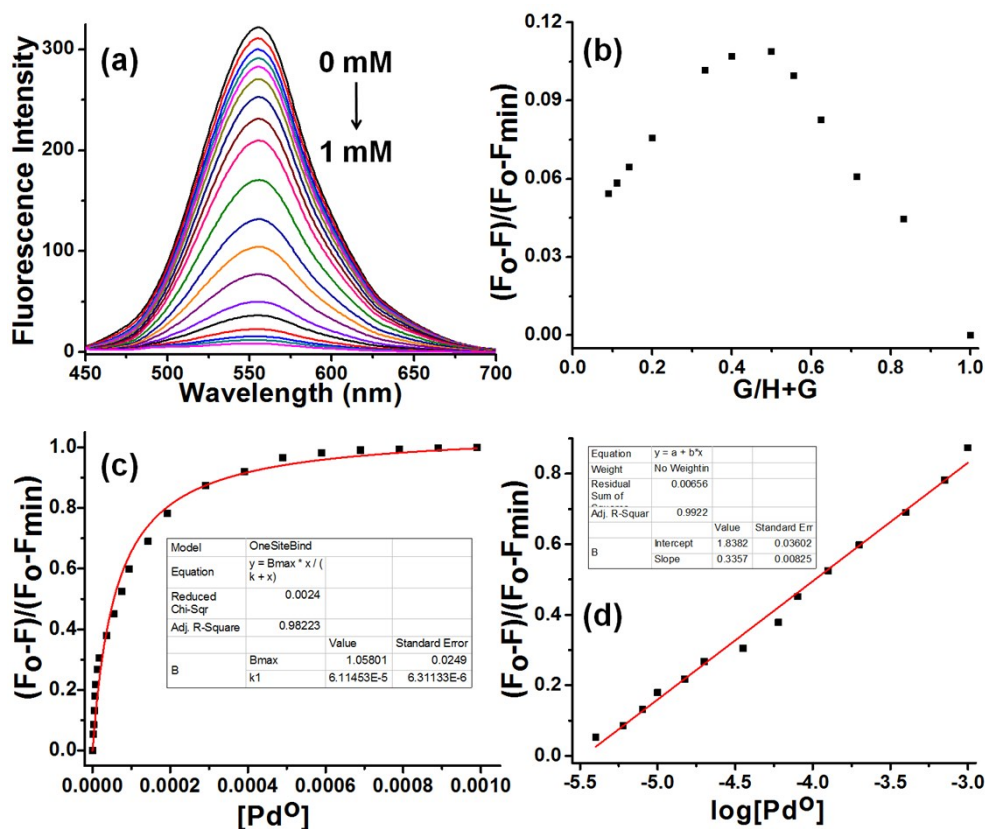


**Figure S6.** (a) Emission spectra (excitation at 425 nm) of receptor **1** (10 μM) upon addition of chloride salt of Pd<sup>0</sup> at pH 7.4 (0.01 M HEPES buffer, 25°C). (b) Assessment of the stoichiometry of the Pd<sup>0</sup> complex of **1** via Job plot analysis;  $[1] + [Pd^0] = 10 \mu M$ , pH 7.4 (0.01 M HEPES buffer), 25°C. (c) Corresponding binding isotherm. (d) A plot of  $(F_o - F)/(F_o - F_{min})$  vs  $\log[Pd^0]$ .

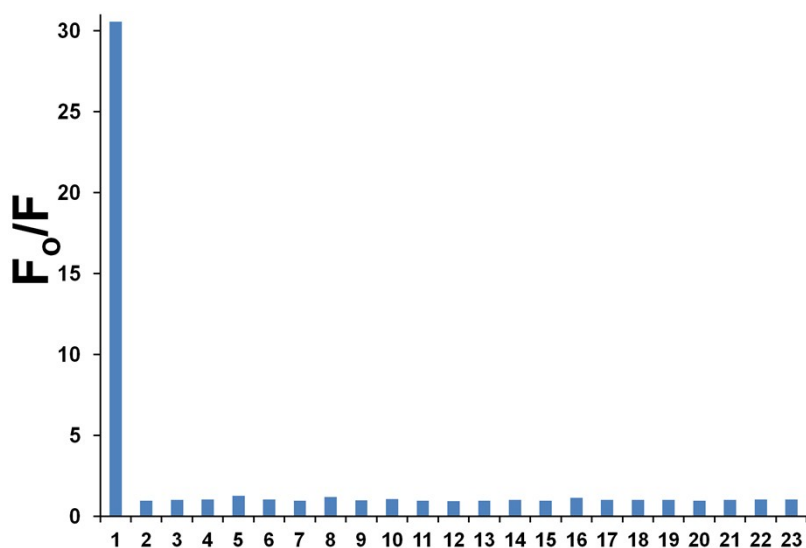


**Figure S7.** Competitive fluorescence response of **1** to various cations at pH 7.4 (0.01 M HEPES) (excitation at 425 nm). Bars represent the addition of 10 equivalent of the Pd<sup>0</sup> and appropriate cation to 10 μM solution of **1** (1:1 H<sub>2</sub>O and Ethanol). (1) No cation, (2) Ca<sup>2+</sup>, (3) Cd<sup>2+</sup>, (4) Co<sup>2+</sup>, (5) Cr<sup>3+</sup>, (6) Cu<sup>2+</sup>, (7) Fe<sup>2+</sup>, (8) Fe<sup>3+</sup>, (9) Hg<sup>1+</sup>, (10) Hg<sup>2+</sup>, (11) K<sup>1+</sup>, (12) Li<sup>1+</sup>, (13) Mg<sup>2+</sup>, (14) Mn<sup>2+</sup>, (15) Na<sup>1+</sup>, (16) Ni<sup>2+</sup>, (17) Pb<sup>2+</sup>, (18) Pt<sup>2+</sup>, (19) Zn<sup>2+</sup>, (20) Zr<sup>2+</sup>, (21) Ba<sup>2+</sup>, (22) Au<sup>1+</sup> and (23) Ag<sup>1+</sup>.

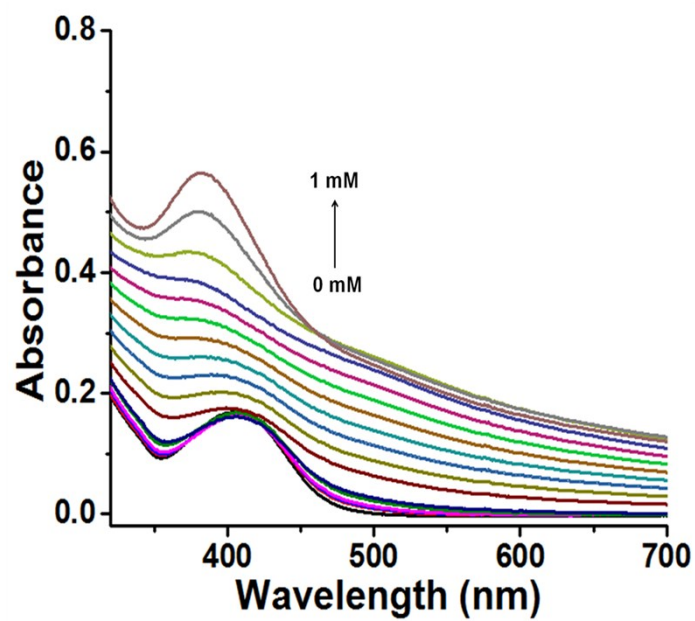


Figure S8. UV/Vis titration of Probe 1 with Pd<sup>2+</sup>.

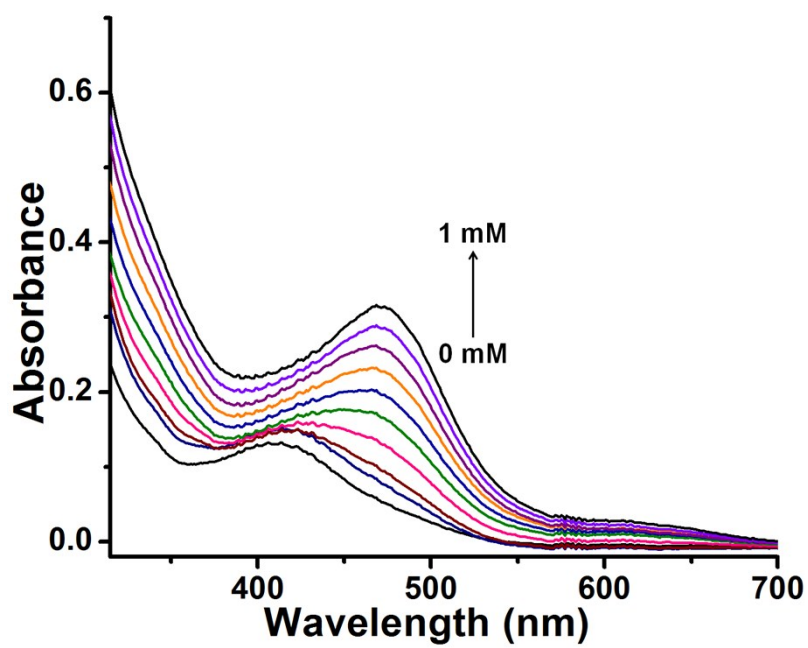
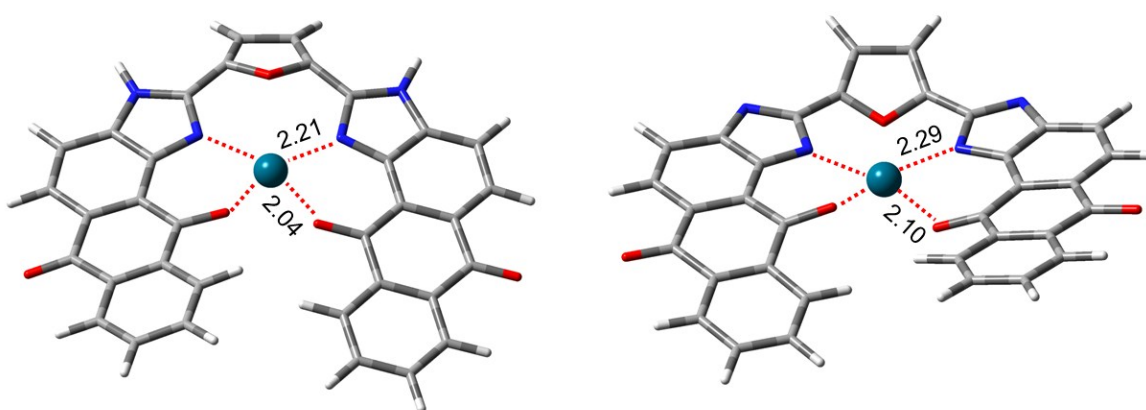


Figure S9. UV/Vis titration of Probe 1 with Pd<sup>0</sup>.

#### 4. Theoretical Calculations

For binding mode analysis, we performed density functional theory calculations. The PBE functional<sup>3</sup> with Grimme's D3 dispersion scheme<sup>4</sup> was employed for geometry optimization. We employed resolution of identity approximation (RI) and rather small basis, 6-31G\* for both Pd<sup>0</sup> and Pd<sup>2+</sup> systems.<sup>5</sup> For Pd atom, the LANL2DZ effective core potential (ECP) basis set was used.<sup>6</sup> The solvent effect was taken into account by using conductor-like screening model.<sup>6</sup> After geometry optimization, we calculated the absorption spectra using M06-2X functional<sup>7</sup> with the polarizable continuum model<sup>8</sup> for implicit water solvent. The geometry optimization was performed using Turbomole 6.4,<sup>9</sup> while the absorption spectra was carried out using the Gaussian09 suite of programs.<sup>10</sup> The results are shown in Figures S10 and S11.



**Figure S10.** The optimized geometries of Pd<sup>2+</sup> (left) and Pd<sup>0</sup> (right) complexes calculated at RI-PBE-D3/6-31G\*/LANL2DZ ECP level of theory.



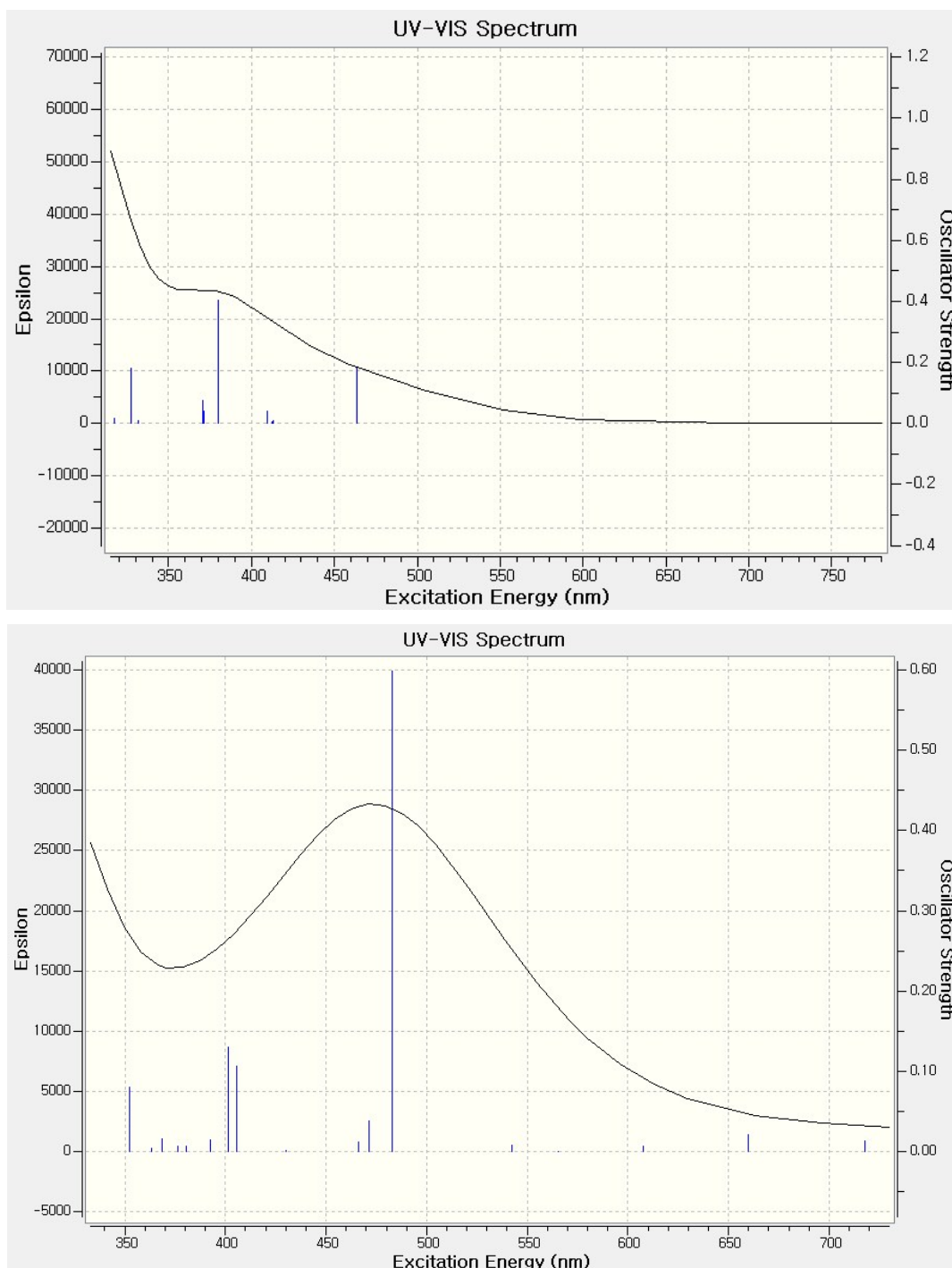


**Figure S11.** Calculated absorption spectra of Pd<sup>2+</sup> (upper) and Pd<sup>0</sup> (lower) complexes calculated at the M06-2X/6-31G\*/LANL2DZ ECP level of theory.

Both Pd<sup>0</sup> and Pd<sup>2+</sup> systems show tetradentate complexes; two oxygen atoms and two nitrogen atoms coordinate to central metal Pd<sup>0</sup> and Pd<sup>2+</sup> atoms. There is small difference between them in coordination distance; somewhat shorter distances are observed in the Pd<sup>2+</sup> complex than in the Pd<sup>0</sup> complex probably because Pd<sup>2+</sup> has more vacant sites to receive lone pair electrons from the donating groups.

## 5. References

- 1 (a) S. Chen, P. Hou, J. W. Foley and S. Song, *RSC Advances*, 2013, **3**, 5591; (b) P. R. Mussini, T. Mussini and S. Rondinini, *Pure & Appl. Chem.*, 1997, **69**, 1007.
- 2 a) K. A. Connors, *Binding Constants: The Measurement of Molecular Complex Stability*, Wiley, New York, **1987**; b) OriginLab 8.0, OriginLab Corporation, Northampton, MA, **2003**. (c) E. Cielen, A. Tahri, K. V. Heyen, G. J. Hoornaert, F. C. De Schryver, N. Boens, *J. Chem. Soc., Perkin Trans, 2*, **1998**, 1573.
- 3 a) J. P. Perdew, K. Burke, M. Ernzerhof, *Phys. Rev. Lett.*, **1996**, *77*, 3865; b) J. P. Perdew, K. Burke, M. Ernzerhof, *Phys. Rev. Lett.*, **1997**, *78*, 1396.
- 4 S. Grimme, J. Antony, S. Ehrlich, *J. Chem. Phys.*, **2010**, *132*, 154104.
- 5 a) G. A. Petersson, A. Bennett, T. G. Tensfeldt, M. A. Al-Laham, W. A. Shirley, J. Mantzaris, *J. Chem. Phys.*, **1988**, *89*, 2193; b) G. A. Petersson, M. A. Al-Laham, *J. Chem. Phys.*, **1991**, *94*, 6081.
- 6 A. Klamt, G. Schuurmann, *J. Chem. Soc. Perkin Trans*, **1993**, *2*, 799.
- 7 Y. Zhao, D. G. Truhlar, *Theor. Chem. Acc.*, **2008**, *120*, 215.
- 8 J. Tomasi, B. Mennucci, R. Cammi, *Chem. Rev.*, **2005**, *105*, 2999.
- 9 TURBOMOLE V6.4 2012; a development of University of Karlsruhe and Forschungszentrum Karlsruhe GmbH: Karlsruhe, Germany, **2007**. Available from <http://www.turbomole.com>.
- 10 M. J. Frisch, G. W. Trucks, H. B. Schlegel, G. E. Scuseria, M. A. Robb, J. R. Cheeseman, G. Scalmani, V. Barone, B. Mennucci, G. A. Petersson, H. Nakatsuji, M. Caricato, X. Li, H. P. Hratchian, A. F. Izmaylov, J. Bloino, G. Zheng, J. L. Sonnenberg, M. Hada, M. Ehara, K. Toyota, R. Fukuda, J. Hasegawa, M. Ishida, T. Nakajima, Y. Honda, O. Kitao, H. Nakai, T. Vreven, J. A. Montgomery Jr., J. E. Peralta, F. Ogliaro, M. Bearpark, J. J. Heyd, E. Brothers, K. N. Kudin, V. N. Staroverov, R. Kobayashi, J. Normand, K. Raghavachari, A. Rendell, J. C. Burant, S. S. Iyengar, J. Tomasi, M. Cossi, N. Rega, J. M. Millam, M. Klene, J. E. Knox, J. B. Cross, V. Bakken, C. Adamo, J. Jaramillo, R. Gomperts, R. E. Stratmann, O. Yazyev, A. J. Austin, R. Cammi, C. Pomelli, J. W. Ochterski, R. L. Martin, K. Morokuma, V. G. Zakrzewski, G. A. Voth, P. Salvador, J. J. Dannenberg, S. Dapprich, A. D. Daniels, Ö. Farkas, J. B. Foresman, J. V. Ortiz, J. Cioslowski, D. J. Fox, Gaussian 09, revision B.01; Gaussian, Inc.: Wallingford CT, **2009**.